

<https://doi.org/10.1038/s43247-025-02143-1>

Extreme drought-heatwave events threaten the biodiversity and stability of aquatic plankton communities in the Yangtze River ecosystems



Jixuan Lyu¹, Yong Shi¹, Tao Liu², Xiaomei Xu¹, Shengjing Liu¹, Guang Yang¹, Dong Peng^{1,3}, Yubing Qu¹, Shuo Zhang², Chonghao Chen¹, Yanxu Zhang^{1,3} & Jianhua Gao^{1,2}✉

Rivers are crucial to biogeochemical cycles, connecting terrestrial, oceanic, and atmospheric systems. However, their ecosystems are increasingly threatened by extreme weather events. Here we used the environmental DNA approach to assess the impact of extreme drought-heatwave events on the aquatic plankton communities of the Yangtze River. We showed that an extreme drought-heatwave event reduced the α diversity of communities, increased their β diversity, and simultaneously simplified and destabilized community network structure. This event also shifted the dominant algae taxa from Bacillariophyta to Cyanobacteria, accompanied by increases in organic carbon and labile organic carbon contents. Globally, temperature rises during this extreme drought-heatwave event are more pronounced in high-latitude regions, likely amplifying impacts on river ecosystem biodiversity and stability. Our findings highlight the vulnerability of river ecosystems to extreme events and underscore the need to mitigate climate change's effects on river ecosystems.

Rivers play an important role in biogeochemical cycles among land, ocean, and atmosphere^{1–3}, yet in recent years, the aquatic ecosystems of rivers worldwide have been directly threatened by human activities such as damming^{4–6}, and are further increasingly affected by climate change-induced extreme weather events, such as heatwaves, droughts, and floods^{7–9}. The frequent occurrence and increased intensity of extreme weather events are detrimental to riverine biota and ecosystem functions and may lead to continuous disturbance of aquatic communities, lowering the resilience of aquatic communities and making it difficult to recover to a stable state, thereby affecting the balance of the entire ecosystem¹⁰. Among extreme weather events, droughts and heatwaves often occur simultaneously due to their similar synoptic circulation anomalies^{11–13}, and the frequency of compound drought-heatwave events is expected to increase tenfold globally under the highest emissions scenario by the late 21st century¹⁴. Compound drought-heatwave events are increasingly regarded as one of the worst climatic stressors to global ecosystem health^{15–17}.

In river ecosystems, aquatic plankton communities are foundational, forming the base of the aquatic food web and contributing to primary production^{18,19}. For example, as the primary producer in aquatic ecosystems,

algae are crucial for the entire ecosystem's carbon dynamics^{20,21}. They not only influence water quality and facilitate material cycles through processes like photosynthesis and decomposition but also serve as indicators of ecosystem health and stability via their diversity and abundance²⁰, which however, could be easily impacted by extreme weather events in terms of biodiversity and stability^{22,23}. Therefore, in the context of global climate change, the response of algae to extreme drought-heatwave events has important consequences for the global carbon cycle, and understanding the impact of extreme drought-heatwave events on the biodiversity and stability of aquatic plankton communities is essential for the long-term conservation and management of river ecosystems. Despite results that broaden our understanding of aquatic communities, most studies only focus on a single taxonomic group (e.g., fish)^{24–26}, and variation in the multitrophic aquatic plankton communities due to extreme drought-heatwave events in a changing global environment, as well as their impact on the carbon cycles of aquatic biospheres, are still incompletely characterized.

In the summer of 2022 (June–August), many countries worldwide experienced extreme heatwaves, including a record-breaking drought-heatwave event in the Yangtze River Basin (Fig. 1a), which led to historically

¹School of Geography and Ocean Science, Ministry of Education Key Laboratory for Coast and Island Development, Nanjing University, Nanjing, Jiangsu Province, China. ²Collaborative Innovation Center of South China Sea Studies, Nanjing University, Nanjing, Jiangsu Province, China. ³Nanjing University, School of Atmospheric Sciences, 163 Xianlin Road, Qixia District, Nanjing, 210023, China. ✉e-mail: jhgao@nju.edu.cn

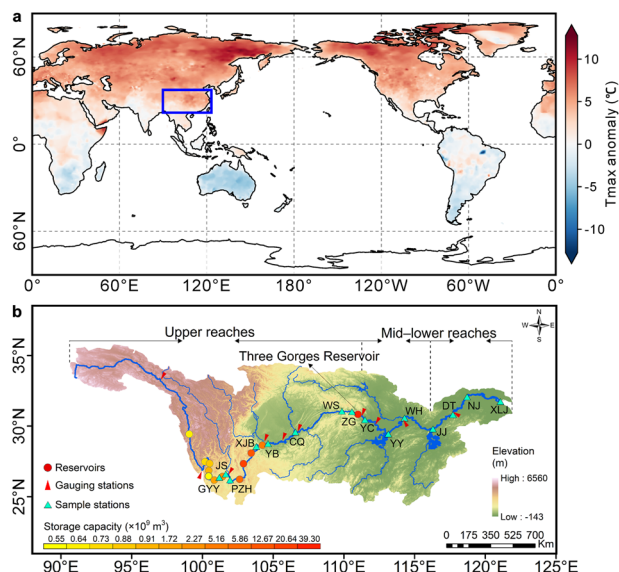


Fig. 1 | Map showing the study area. a Average surface air temperature anomaly (°C) for June–August 2022 worldwide, relative to the average for the 1991–2020 reference period. The data are obtained from the National Oceanic and Atmospheric Administration (NOAA, <https://psl.noaa.gov>). The blue square represents the location of the Yangtze River basin. **b** Locations of dam-associated reservoirs, gauging stations, and sampling stations in the Yangtze River. The water level, water discharge, sediment load, precipitation, and air temperature of the Yangtze River Basin are provided in Supplementary Figs. 1–4.

low water levels in the middle-lower reaches (Supplementary Fig. 1)^{27,28}. This offers a notable case study that examines the impacts of extreme drought-heatwave events on aquatic plankton communities in river ecosystems. The Yangtze River is the third-longest river in the world and is becoming an artificially regulated river due to damming, where its ecosystem is regularly affected by dams^{29–31}. Yet, under the context of dam regulation, no research has been done to study the impact of extreme drought-heatwave events on aquatic plankton communities in the Yangtze River Basin.

To bridge the aforementioned understanding gap, we analyzed multitrophic groups, including Eukaryotic algae, Animalia, Fungi, Protozoa, Cyanobacteria, and Bacteria, using the environmental DNA (eDNA) approach from suspended particulate matter sampled in the Yangtze River Basin (Fig. 1). We selected three sampling periods to represent distinct hydrological conditions. The water drainage/flood control period (hereafter referred to as the water drainage period, represented by July 2021) and water storage period (October 2021) were sampled during a normal hydrological year, while the extreme drought-heatwave event period (August 2022) marked by severe hydrological and meteorological anomalies despite being in the water drainage period within the wet season (May–October). The main objectives of this work are to show: (a) the impact of extreme drought-heatwave events on the composition and stability of river ecosystems, (b) the variation in algae communities and its knock-on implications for the carbon budget and the carbon cycle, and (c) a reference for other large and rapidly changing river systems.

Results and discussion

Here using the Yangtze River Basin as an example, we examine shifts in the composition, spatial distribution, biodiversity, and network structure of aquatic plankton communities during the water drainage, water storage, and extreme drought-heatwave event periods. Our findings highlight the dynamic and sensitive responses of aquatic ecosystems to hydrological and climatic variations, reflecting the intricate interactions within these systems under environmental stress. Given the critical role of biodiversity and community composition in

ecosystem stability and biogeochemical cycling, understanding these responses is crucial for advancing our knowledge of ecosystem resilience, carbon cycles, and climate change.

Composition and spatial pattern of aquatic plankton communities

All OTUs (Operational Taxonomic Units) were assigned to 11 kingdoms, 64 Phylum, 148 classes, 244 orders, 313 families, 509 genera, and 1087 species. A total of 309580 reads and 708 OTUs in Eukaryotic Algae (mean 7938 reads and 230 OTUs per sample), 343261 reads and 268 OTUs in Animalia (mean 8802 reads and 45 OTUs per sample), 65678 reads and 524 OTUs in Fungi (mean 1684 reads and 93 OTUs per sample), 112838 reads and 1681 OTUs in Protozoa (mean 2893 reads and 204 OTUs per sample; excluding Eukaryotic algae), 173983 reads and 181 OTUs in Cyanobacteria (mean 4461 reads and 44 OTUs per sample), and 71675 reads and 502 OTUs in Bacteria (mean 1838 reads and 95 OTUs per sample; excluding Cyanobacteria) were detected by the eDNA approach after stringent quality filtering.

The most abundant taxa were Mediophyceae and Chlorophyceae in Eukaryotic Algae, Maxillopoda and Bivalvia in Animalia, Perkinsidae in Protozoa, unclassified_k_Fungi in Fungi, Synechococcales in Cyanobacteria, and c_unclassified_d_Bacteria in Bacteria across the Yangtze River Basin. The distribution and abundance of community composition in different samples and periods were shown in Supplementary Fig. 5.

The qPCR results and abundance in Eukaryotic algae, Animalia, Fungi, Protozoa, Cyanobacteria, and Bacteria were shown in Fig. 2. The average proportions of Eukaryotic algae were $26 \pm 9\%$, $28 \pm 18\%$, and $23 \pm 11\%$ during the water drainage, water storage, and extreme drought-heatwave periods, respectively; the average proportions of Animalia were $19 \pm 14\%$, $43 \pm 27\%$, and $29 \pm 18\%$ during the three periods, respectively; the average proportions of Fungi were $9 \pm 11\%$, $3 \pm 2\%$, and $4 \pm 6\%$ during the three periods, respectively; the average proportions of Protozoa were $20 \pm 14\%$, $8 \pm 6\%$, and $4 \pm 4\%$ during the three periods, respectively; the average proportions of Cyanobacteria were $19 \pm 12\%$, $13 \pm 11\%$, and $32 \pm 10\%$ during the three periods, respectively; the average proportions of Bacteria were $7 \pm 6\%$, $6 \pm 4\%$, and $8 \pm 4\%$ during the three periods, respectively.

The ranges of total gene quantity of aquatic plankton communities were 1.4×10^9 – 1.7×10^{10} copies g^{-1} (copies per gram of suspended particulate matter), 4.9×10^9 – 1.5×10^{11} copies g^{-1} , and 5.9×10^9 – 1.0×10^{11} copies g^{-1} during the water drainage, water storage, and extreme drought-heatwave periods, respectively, with the average gene quantity in both the water storage and extreme periods being higher than that in the water drainage period ($P = 0.002$ and 0.002 , respectively, by the Kruskal-Wallis test).

Among the algae communities (Fig. 3), Bacillariophyta accounted for $20 \pm 13\%$, $29 \pm 20\%$, and $14 \pm 12\%$ during the water drainage, water storage, and extreme drought-heatwave periods, respectively; Chrysophyta accounted for $2 \pm 2\%$, $1 \pm 2\%$, and $1 \pm 1\%$ during the three periods, respectively; Dinophyta accounted for $4 \pm 4\%$, $2 \pm 1\%$, and $1 \pm 1\%$ during the three periods, respectively; Chlorophyta accounted for $20 \pm 10\%$, $17 \pm 8\%$, and $19 \pm 9\%$ during the three periods, respectively; Cryptophyta accounted for $13 \pm 5\%$, $18 \pm 13\%$, and $7 \pm 4\%$ during the three periods, respectively; Cyanophyta accounted for $41 \pm 16\%$, $32 \pm 18\%$, and $59 \pm 12\%$ during the three periods, respectively. In addition, total algae gene quantity showed a significant positive correlation ($P < 0.001$) with particulate organic carbon (POC) and labile POC contents (Fig. 4).

Biodiversity, network structure, and environmental drivers of aquatic plankton communities

Venn diagrams showed that the unique number of OTUs peculiar to the water storage period (178 OTUs) and extreme period (129 OTUs) was smaller than that in the water drainage (937 OTUs) (Fig. 2d). Compared with the water drainage period in the normal year, the extreme drought-heatwave event had an impact on the whole basin, leading to 79% and 85% decreases in the number of distinct OTUs in the upper and mid-lower reaches, respectively.

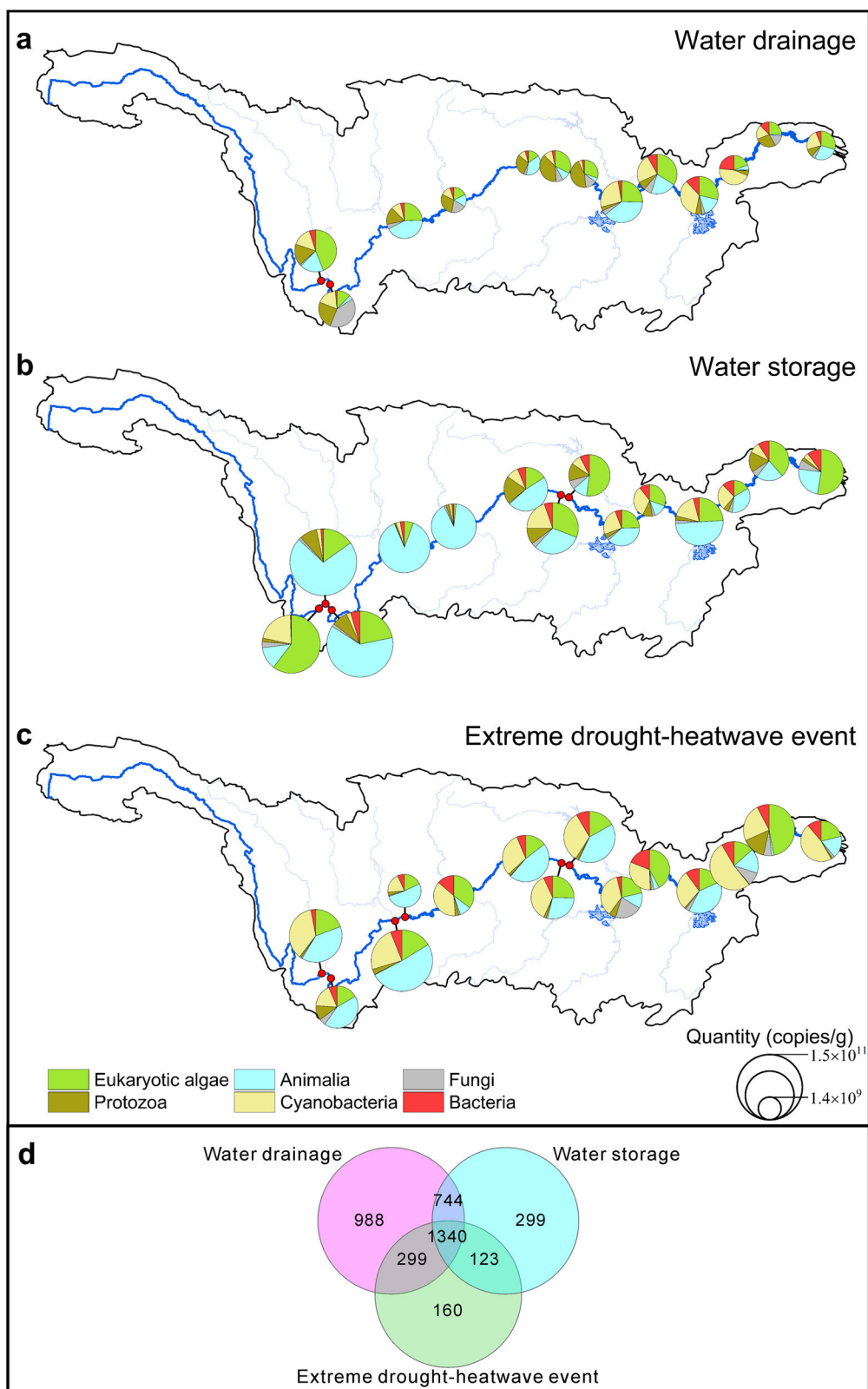


Fig. 2 | Spatial distribution of aquatic plankton communities in the Yangtze River Basin. a water drainage period. **b** water storage period. **c** extreme drought-heatwave event period. Symbols are scaled by the gene quantity and presented as the mean of triplicate samples. **d** numbers of shared and unique OTUs during the three periods.

The Good's coverage index from Eukaryotic algae to Bacteria communities ranged from $92.4 \pm 4.7\%$ to $99.9 \pm 0.1\%$ for the samples, confirming that the current profiles well represented the primary communities. Eukaryotic algae, Bacteria, Fungi, and Protozoa showed a significant decrease from the water drainage to the extreme drought-

heatwave event periods in the Chao1 richness index, Ace richness index, and Shannon's diversity index (Fig. 5), while the β diversity of Eukaryotic algae, Protozoa, Fungi, Bacteria, and Cyanobacteria showed significant increases from the water drainage to the extreme drought-heatwave event periods (Fig. 6), whereas both the α and β

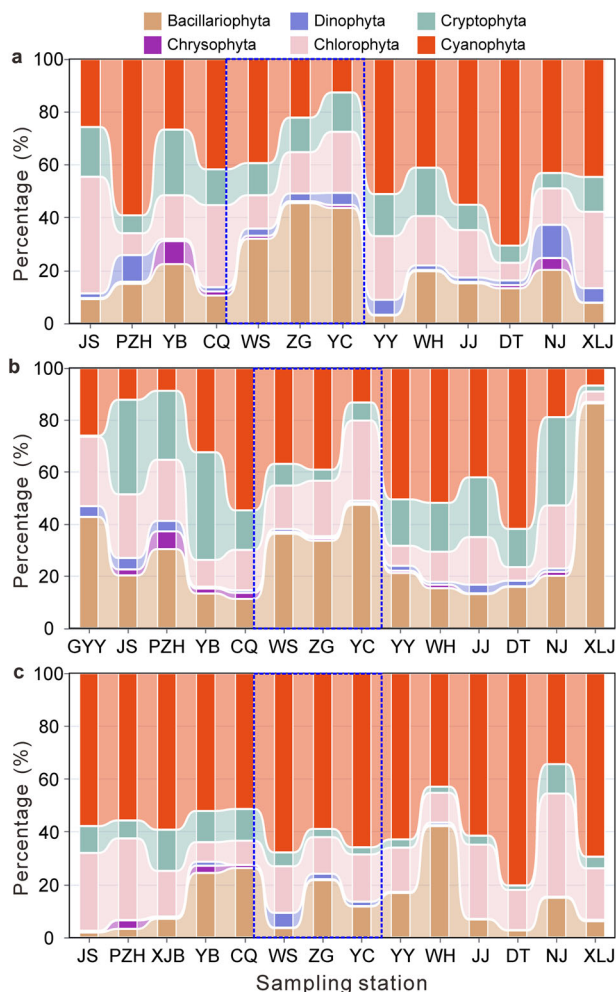


Fig. 3 | Composition of algae community. **a** water drainage period. **b** water storage period. **c** extreme drought-heatwave event period. The blue dotted boxes in stations WS, ZG, and YC represent the Three Gorges Reservoir impact areas.

diversity of Animalia showed no significant changes among the three periods.

We constructed univariate correlation networks to explore relationships between taxa (Supplementary Fig. 6) and uncover the underlying structural attributes of taxa interactions (Fig. 7). Compared with the water drainage period, the edge number, average neighbor number, density, clustering coefficient, and modularity of the community network synergistically decreased during the extreme drought-heatwave event period (Fig. 7).

Based on the partial Mantel test, we explored associations of hydro-geochemical variables (including water temperature, dissolved oxygen, total phosphorus, total nitrogen, ammonia nitrogen, suspended sediment concentration, pH, chemical oxygen demand, and biochemical oxygen demand) with aquatic plankton communities in the water drainage, water storage, and extreme drought-heatwave event periods (Fig. 8). The result indicated that water temperature was a consistently strong driver affecting aquatic communities across all three periods. During the water drainage, water storage, and extreme drought-heatwave event periods, the average water temperatures of sampling stations in the Yangtze River were 25.2 ± 2.0 °C, 22.7 ± 1.6 °C, and 28.6 ± 2.7 °C, respectively. The average water temperature during the extreme drought-heatwave period was significantly higher compared to the water drainage ($P = 0.003$) and water storage ($P < 0.001$) periods, with increases of 3.4 ± 2.0 °C and 5.9 ± 1.9 °C, respectively (Supplementary Fig. 7).

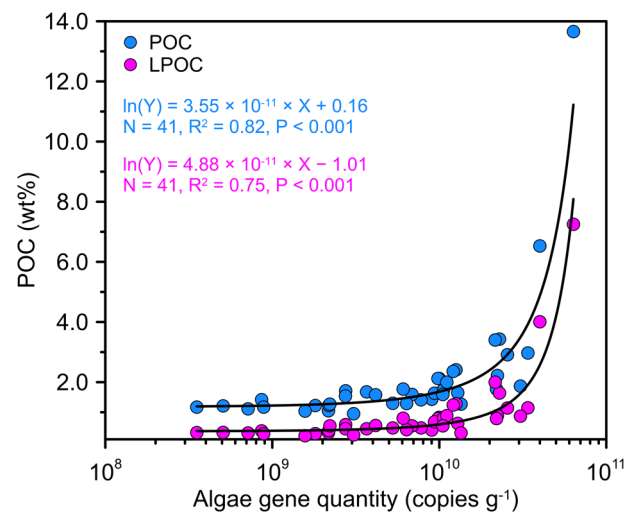


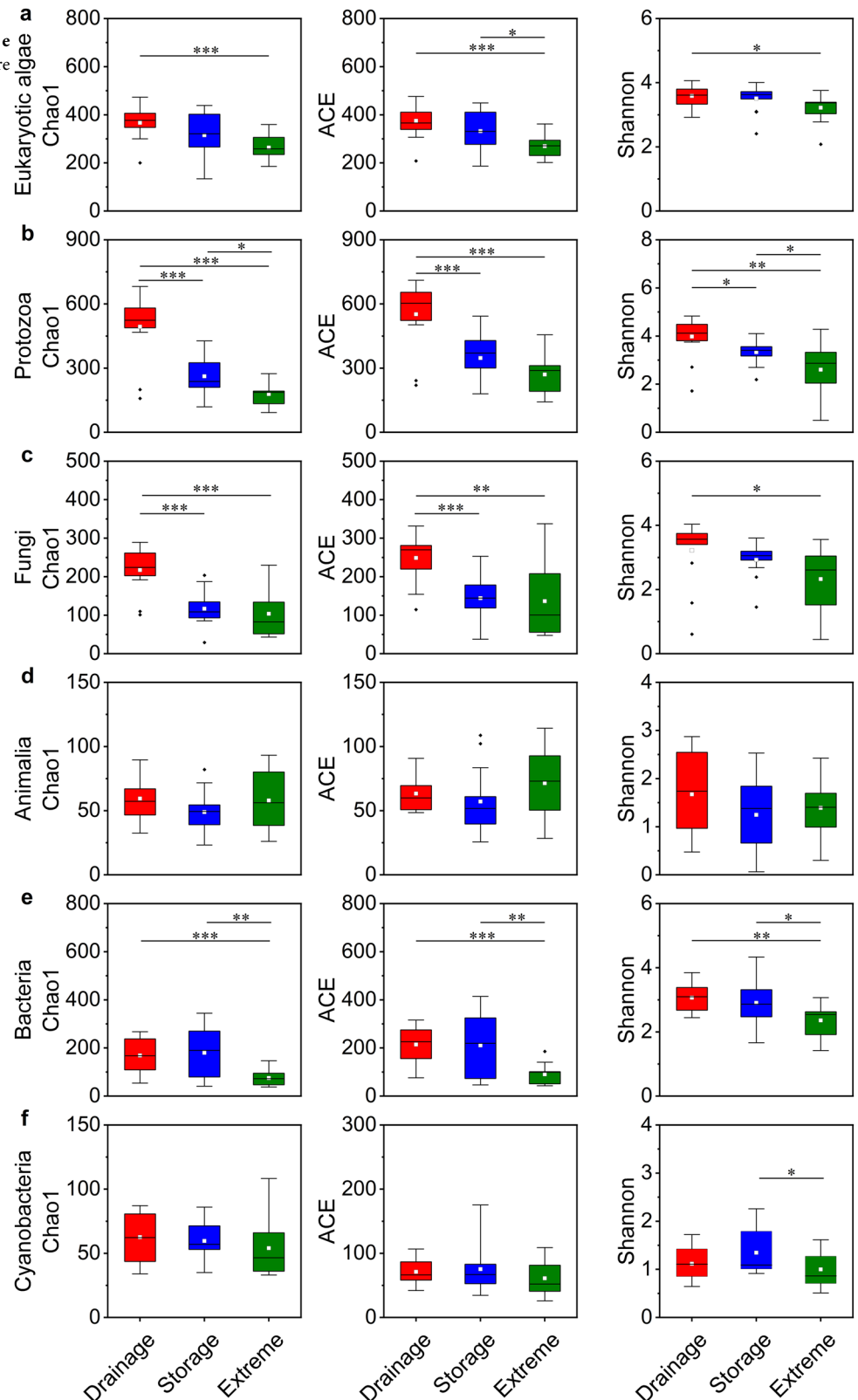
Fig. 4 | Relationships between POC and algae contents. The data are from all sample stations during the water drainage, water storage, and extreme drought-heatwave event periods. Data points are presented as the mean of duplicate samples. Error bars are smaller than symbol sizes and not shown.

Altered biodiversity and reduced stability in aquatic plankton communities under the extreme drought-heatwave condition. Extreme drought-heatwave events increase environmental stress (for instance, water temperature can impact communities through several ecological mechanisms including metabolic regulation, community composition shift, and dissolved oxygen dynamics^{32–35}), causing many species to be unable to adapt to these harsh conditions and be eliminated (unique OTUs and α diversity), and increasing the species composition differences between regions (β diversity)³⁶. Reduced α diversity could weaken the ecosystem's ability to recover from further environmental changes and disturbances^{37,38}, while increased β diversity indicates greater differences in ecosystem functions between regions. This might help river systems maintain certain functions in the face of environmental changes such as heatwaves but could also lead to increased system variability, reducing the overall stability of ecosystems³⁹.

Although water regulation and extreme drought-heatwave events drove variations in taxa (Figs. 5 and 6), Protozoa and Fungi had a stronger response (e.g., Chao1 richness index) to the water storage than other taxonomic groups (Fig. 5b, c), while Eukaryotic Algae, Protozoa, Fungi, and Bacteria were all driven by the extreme drought-heatwave event (e.g., Shannon's diversity; Fig. 5a–c and e), indicating that the extreme drought-heatwave event had a greater impact on aquatic communities than water regulation for its broader influence on aquatic community composition. In this study, Animalia exhibited stability and had no significant response to either the water regulation or extreme drought-heatwave event (Figs. 5d and 6d). Compared with microbial communities in lower trophic levels, such as Fungi and Bacteria, Animalia often possesses a greater adaptive capacity to cope with unfavorable conditions and environmental stressors^{40–42}. This resilience is attributed to their behavioral and physiological plasticity, such as mechanisms like thermal acclimation, physiological adjustments, and metabolic adaptations, enabling them to survive elevated water temperatures and hypoxic environments^{43–45}.

The variation in biodiversity led to changes in taxa interactions, which in turn changed the stability of the community network (Fig. 7). Under the pressure of extreme drought-heatwave events, the lower edge number, average neighbor, density, and clustering coefficient (Fig. 7a–d) of aquatic plankton communities indicated reduced connectivity and collaboration within the ecosystem, potentially leading to decreased resilience and efficiency in resource distribution^{46,47}. In addition, lower modularity (Fig. 7e) reflected less distinct community structures, which can affect the ecosystem's ability to maintain functional integrity and adaptability under stress⁵.

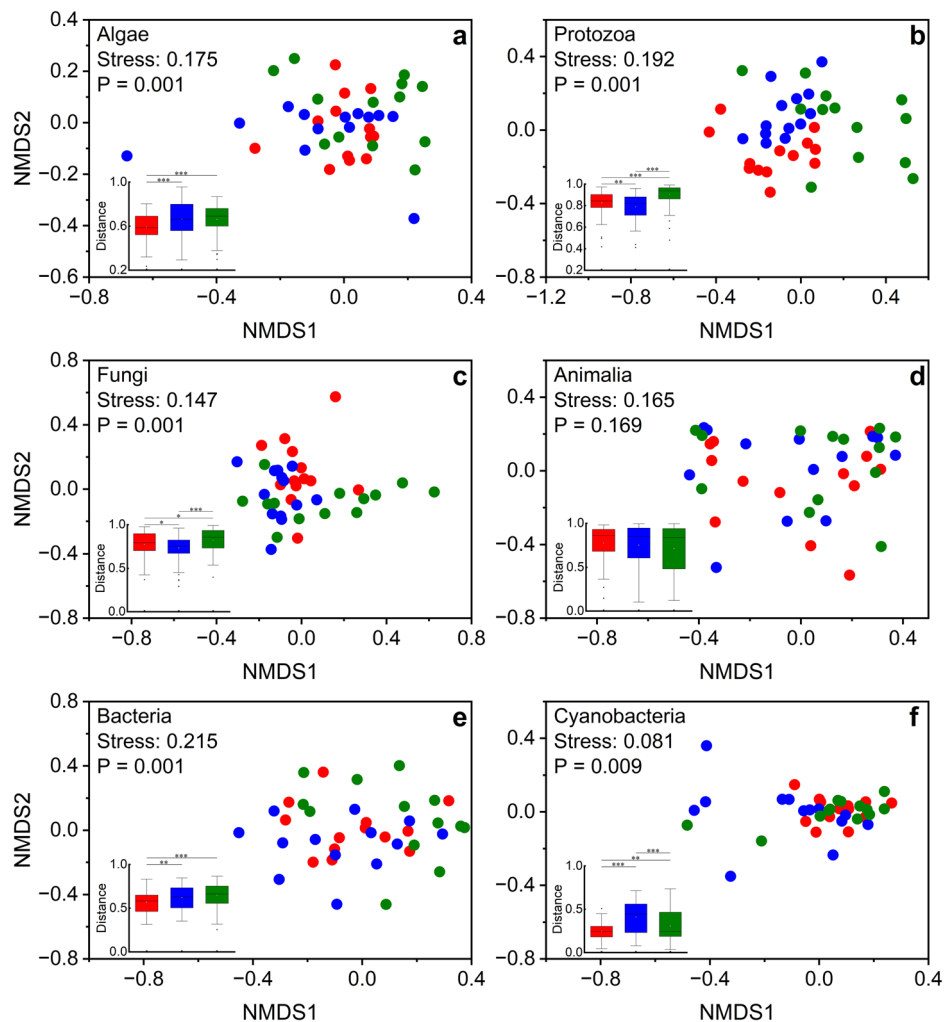
Fig. 5 | Discrimination for the α diversity. **a** Eukaryotic algae. **b** Protozoa. **c** Fungi. **d** Animalia. **e** Bacteria. **f** Cyanobacteria. Significant differences are studied using the Kruskal-Wallis test with FDR multiple testing correction. * $P < 0.5$; ** $P < 0.01$; *** $P < 0.001$.



Variation in algae communities caused by the extreme drought-heatwave event affecting carbon cycle. The extreme drought-heatwave event affected the biodiversity and stability of aquatic plankton communities, which could bring important effects that we should pay close attention to. As the primary producer in aquatic ecosystems, algae contribute immensely to the fixation of atmospheric CO_2 through

photosynthesis, playing a critical role in the carbon dynamics of rivers^{48,49}, thus changes in the composition and gene quantity of algae communities due to the extreme drought-heatwave event have effects on the carbon cycle and the carbon budget. In river systems, energy supply (as light or nutrient inputs) and flow stability are the two major drivers for riverine primary productivity⁵⁰. The extreme drought-heatwave event lowered

Fig. 6 | Discrimination for the β diversity. **a** Eukaryotic algae. **b** Protozoa. **c** Fungi. **d** Animalia. **e** Bacteria. **f** Cyanobacteria. Ordination plots of community structure based on Bray-Curtis dissimilarity matrices. Significant differences were studied by Adonis with the Monte Carlo 999 permutations test; the close dots in the ordination space indicate that each shares a larger percentage of taxa with the other. Boxplots showing the pairwise comparison of the dissimilarity of community structure among the three periods. significant differences were investigated using the one-way ANOVA followed by post-hoc Bonferroni test. * $P < 0.05$; ** $P < 0.01$; *** $P < 0.001$.



water levels, prolonged water retention time (reflected as lower water discharge, Supplementary Fig. 3), decreased water turbidity (Supplementary Fig. 8), and provided more light supply, thus promoting nutrient availability (higher TN concentration⁵¹) and photosynthetic activity among primary producers^{6,41,52,53}.

Reservoir interception changed the dominant taxa in the Three Gorges Reservoir in the normal year in both water drainage and water storage periods (Fig. 3a, b) — from predominantly Cyanobacteria at station CQ to predominantly Bacillariophyta at station YC, and then the dominant taxa downstream of the Three Gorges Reservoir (from station YY to station XLJ) was changed to Cyanobacteria again. Compared with the water drainage period, the dominant taxa in the extreme drought-heatwave event was Cyanobacteria throughout the whole basin, covering up the impact of reservoirs on altering dominant taxa. Among river algae, diatoms are efficient primary producers with high nutritional value, supporting zooplankton and primary consumers, thus enhancing biodiversity and ecosystem productivity^{54,55}. In contrast, Cyanobacteria thrive in warm and stagnant waters with elevated TN/TP ratios, producing toxins like microcystins that harm aquatic life and reduce herbivore palatability^{32,56}. This shift in the dominant taxa of algae can decrease primary consumer populations, reduce biodiversity, and disrupt community structure, making ecosystems more vulnerable to environmental changes^{57,58}.

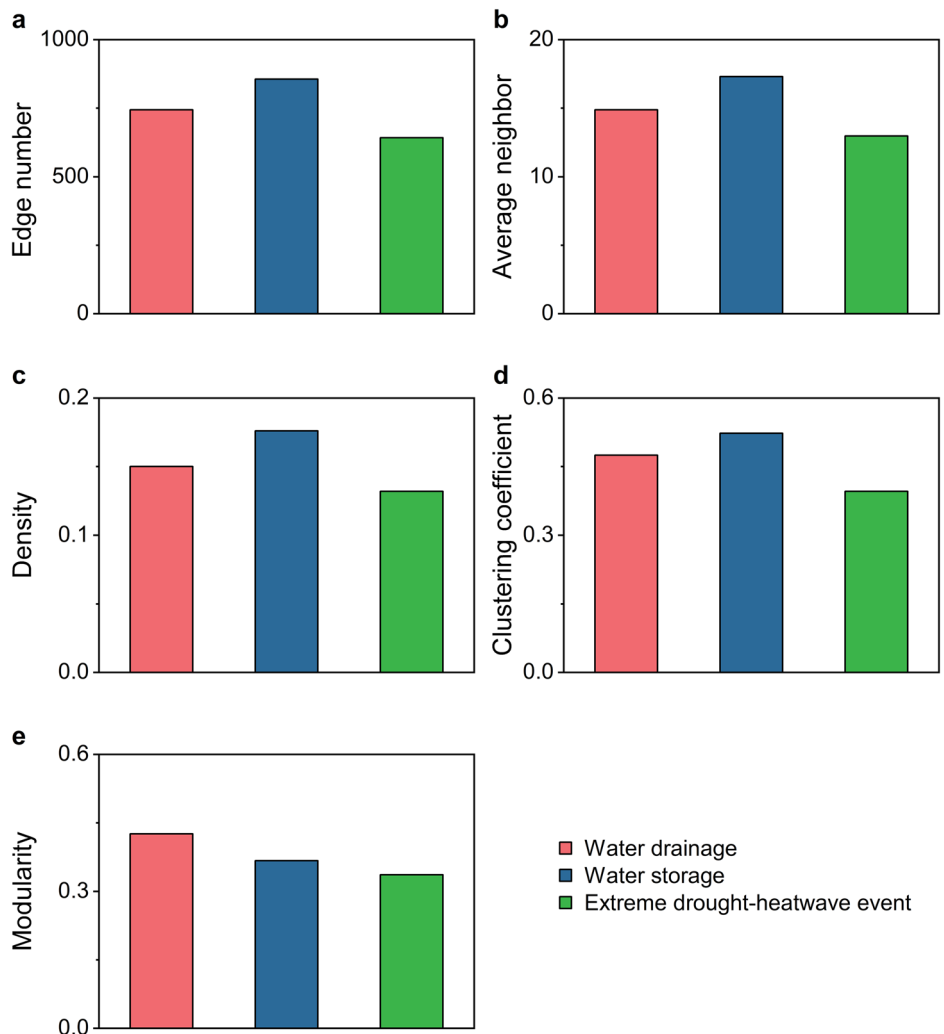
The extreme drought-heatwave event changed not only the composition of algae communities but also the algae gene quantity. Compared to the water drainage period in the normal year, the extreme drought-heatwave event led to a significant increase in algae gene quantity (an 11-fold increase in gene quantity, $P = 0.02$), POC content ($31 \pm 22\%$, $P = 0.002$), and labile

POC proportion of total POC ($18 \pm 8\%$, $p < 0.001$) throughout the whole basin. In addition, algae gene quantity showed a significant positive correlation with POC content (Fig. 4), as well as labile POC content that can be remineralized and decomposed more readily, indicating the dominant role of algae in contributing to POC content. The increase in algae gene quantity and the shift of dominant algae taxa driven by the extreme drought-heatwave event were detrimental to carbon storage. Accordingly, the succession of dominant taxa and the increase in labile POC proportion triggered by the extreme drought-heatwave event could affect the biodiversity and stability of the ecosystem and thus likely change biogeochemical cycles in the Yangtze River Basin.

Implications of changes in aquatic communities for global rivers.

Our results showed that this extreme drought-heatwave event reduced biodiversity and stability in aquatic communities of the Yangtze River Basin, which highlighted the riverine ecosystem's vulnerability to extreme weather events, yet, this extreme drought-heatwave event occurred on a global scale, and the variation in the biodiversity and stability of aquatic communities could occur in other regions worldwide as well. In the climate system, extreme drought-heat events drive changes in air temperature and precipitation, which in turn affect hydrological conditions in the river system. These alterations lead to shifts in the biodiversity and structural stability of riverine aquatic communities, as well as the riverine carbon cycle. Furthermore, changes in the river system can have cascading effects on the coastal ecosystem, which could feedback to the climate system, creating a complex interplay between riverine, coastal, and atmospheric processes⁵⁹ (Fig. 9).

Fig. 7 | Network structure properties for eukaryotic aquatic plankton communities. **a** Edge number. **b** average number of neighbors. **c** density. **d** clustering coefficient. **e** modularity.



During the extreme drought-heatwave event in 2022, although the temperature increase in the Yangtze River Basin was not the most significant (Supplementary Fig. 9a), the biodiversity and stability of aquatic plankton communities were severely negatively affected. With the rise of latitude, temperature increase became greater (Supplementary Fig. 9a), and thus the impact of the extreme drought-heatwave event on the river ecosystems was likely to be amplified. In addition, the fastest temperature growth currently occurs at 70°–80°N (reflected as the biggest slope of the fitted curve, Supplementary Fig. 9b). Heatwave events and rising temperatures may have more severe and lasting impacts on high-latitude regions (high-latitude amplification), such as the Arctic, where permafrost melting could release greenhouse gases and destabilize carbon reserves, exacerbating global warming^{60–62}. This process creates feedback loops that further influence the river system (Fig. 9). Given these vulnerabilities, these issues warrant heightened global attention and action.

The evidence from various river basins worldwide underscores the critical need for global awareness and action to protect riverine biodiversity and stability from the threats posed by extreme weather events^{4,63,64}. Under the context of global warming, the frequency and intensity of extreme events are increasing. A recent study suggested that events similar to those that occurred in 2022 could happen once every 8.5 years rather than the current possibility of once every 76,000 years⁶⁵. This will substantially increase the vulnerability of river ecosystems and may lead to trending changes in the river ecosystem (e.g., during the Millennium Drought in Australia, some rivers failed to recover to pre-drought flow regimes, resulting in irreversible ecosystem changes¹⁶). Effective strategies that integrate ecological needs and

promote sustainable water use are essential to address future aquatic ecosystem challenges posed by extreme weather.

Methods

Regional settings

The Yangtze River is 6300 km long and covers a basin area of around $1.8 \times 10^6 \text{ km}^2$ (Fig. 1). It is geographically divided into upper, middle, and lower reaches. The upper reaches, extending from the Qinghai-Tibetan Plateau to Yichang city, are characterized by mountainous topography with high relief at elevations over 3000 m and mainly distributed with Paleozoic carbonate rocks, Mesozoic sedimentary and igneous rocks. The major tributaries of the upper reaches include the Yalongjiang, Minjiang, Jialingjiang, and Wujiang rivers. The middle-lower reaches mainly consist of riverine plains, and are overlain by the Paleozoic marine, Mesozoic sedimentary rocks, and Quaternary loose sediments of fluvial and lacustrine facies, where the Dongting and Poyang lakes and the Hanjiang River interact closely with the mainstream. Controlled by the Asian monsoon, the annual precipitation in the basin generally ranges from <500 mm in the source region to >1600 mm yr^{-1} in the middle-lower reaches. In the Yangtze River Basin, the wet season typically extends from May to October, while the dry season covers November through the following April.

The Three Gorges Dam is currently the biggest hydropower project in the world, impounded in 2003. In terms of water regulation within a year, the TGR is the most typical for the overall three periods (Fig. 10). Drainage period (January–June): to supply water for the lower reaches and prepare for the wet season, the water level of the TGR is lowered to 145 m; flood control

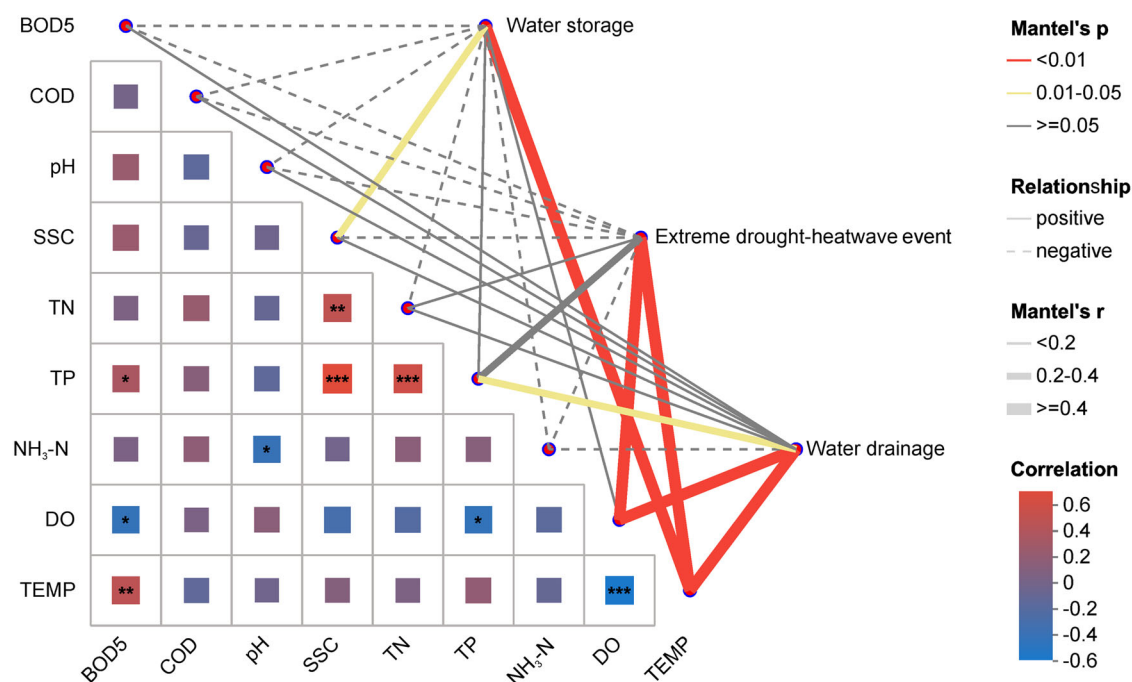


Fig. 8 | Relationships between the hydrogeochemical variables (Euclidean distance) and water drainage, water storage, and extreme drought-heatwave event period (Bray-Curtis distance) revealed by the Mantel test. Edge width corresponds to Mantel's r value, and the edge color denotes statistical significance. Pairwise correlations of these variables are shown with a color gradient denoting

Spearman's correlation coefficient. * $p < 0.05$; ** $0.001 < p < 0.01$; *** $p < 0.001$. TEMP: water temperature; DO: dissolved oxygen; NH₃-N: ammonia nitrogen; TP: total phosphorus; TN: total nitrogen; SSC: suspended sediment concentration; COD: chemical oxygen demand; BOD5: biochemical oxygen demand.

period (June–September): in this stage, the TGR generally operates at the flood control level of 145 m, keeping flood water storage capacity to retain possible floods; storage period (September–December): in this stage, the TGR began to store more incoming water and gradually raised the water level to 175 m to ensure shipping, water replenishment, and power generation.

Sampling

Suspended particulate matter (SPM) was collected within the Yangtze River Basin in July 2021 (13 sampling stations), October 2021 (14 sampling stations), and August 2022 (14 sampling stations), respectively (Fig. 1b). July, August, and October are all in the wet season. During the wet season, the Yangtze River supplies over 86% of the annual sediment load to the East China Sea (MWRC, 1961–2022), suggesting our samples are representative of the majority of POC exported by the Yangtze River.

Sub-surface water samples (0.5 m underwater, 150 L total) were collected from a cross-section in the main channel using acid-washed 25-L polyethylene samplers at each station, and SPM subsequently was recovered by filtering the water under pressure through pre-combusted (450 °C for 3 h) glass fiber filters (nominal pore size: 0.7 µm, Whatman GF/F). All the filtered samples were freeze-dried and stored at -20 °C for further analysis.

DNA extraction, polymerase chain reaction (PCR) amplification, sequencing, and quantitative PCR (qPCR) analysis

Total microbial genomic DNA was extracted from SPM samples using the E.Z.N.A.® soil DNA Kit (Omega Bio-tek, Norcross, GA, USA) following the manufacturer's instructions. The quality and concentration of DNA were determined by 1.0% agarose gel electrophoresis and a NanoDrop® ND-2000 spectrophotometer (Thermo Scientific Inc., USA) and kept at -80 °C before further use. The V4 region of the 18S rRNA gene was amplified with primer pairs 3NDF (5'-GGCAAGTCTGGTGCCAG-3') and V4-euk-R2R (5'-ACGGTATCTRATCCTCTTCG-3'), which were designed to broadly capture eukaryotic diversity⁶⁶; target fragments of the 16S rRNA gene were

amplified with primer pairs CYA359F (5'-GGGAATTTTCG-CAATGGG-3') and aCYA781R (5'-GACTACTGGGGTATCTAATCC-CATT-3') to identify cyanobacteria⁶⁷, by an ABI GeneAmp® 9700 PCR thermocycler (ABI, CA, USA). The PCR reaction mixture including 4 µL 5 × Fast Pfu buffer, 2 µL 2.5 mM dNTPs, 0.8 µL Forward primer (5 µM), 0.8 µL Reverse primer (5 µM), 0.4 µL Fast Pfu polymerase, 10 ng of template DNA, and ddH₂O to a final volume of 20 µL. PCR amplification cycling conditions were composed of initial denaturation at 95 °C for 3 min, followed by 35 cycles of denaturing at 95 °C for 30 s, annealing at 55 °C for 30 s, and extension at 72 °C for 45 s, with a final extension at 72 °C for 10 min. All samples were amplified in triplicate. The PCR product was extracted from 2% agarose gel and purified using the AxyPrep DNA Gel Extraction Kit (Axygen Biosciences, Union City, CA, USA) according to the manufacturer's instructions and quantified using Quantus™ Fluorometer (Promega, USA). Purified amplicons were pooled in equimolar amounts and paired-end sequenced on an Illumina MiSeq platform (Illumina, USA).

The DNA copy numbers of eukaryotes and bacteria in the SPM samples were quantified by qPCR using the primers of 3NDF_V4-euk-R2R and CYA359F_aCYA781R, respectively. qPCR reactions were performed in triplicate, using the Real-Time PCR Detection System. Each multiplex reaction was performed in a 20 µL volume comprising 10 µL 2X ChamQ SYBR Color qPCR Master Mix, 0.8 µL each primer (5 µM), 0.4 µL 50 X ROX Reference Dye 1, 2 µL DNA template, and 6 µL ddH₂O. The qPCR amplification program consisted of an initial denaturation step at 95 °C for 3 min, followed by 40 cycles at 95 °C for 5 s, 58 °C for 30 s, and 72 °C for 60 s. Melting curve and agarose gel electrophoresis analysis were used to confirm the specificity of the amplifications. Standard curves were created using 10-time serial dilutions of plasmids, with correlation coefficients of $R^2 > 0.99$ and amplification efficiencies between 99–108%. The DNA copies in the diluted DNA solution standard were calculated by the following equation: the number of copies per microliter (copies µL⁻¹) = DNA concentration (ng µL⁻¹) × $10^{-9} \times 6.02 \times 10^{23}$ (mol⁻¹) / [660 × genome size (bp)]. The qPCR data was expressed as DNA copies per gram of suspended particulate matter (unit,

Fig. 9 | Interactive relationships among the climate system, river system, and coastal ecosystem. This figure shows the interactions among different environmental components and how they are influenced by extreme drought-heatwave events and water regulation.

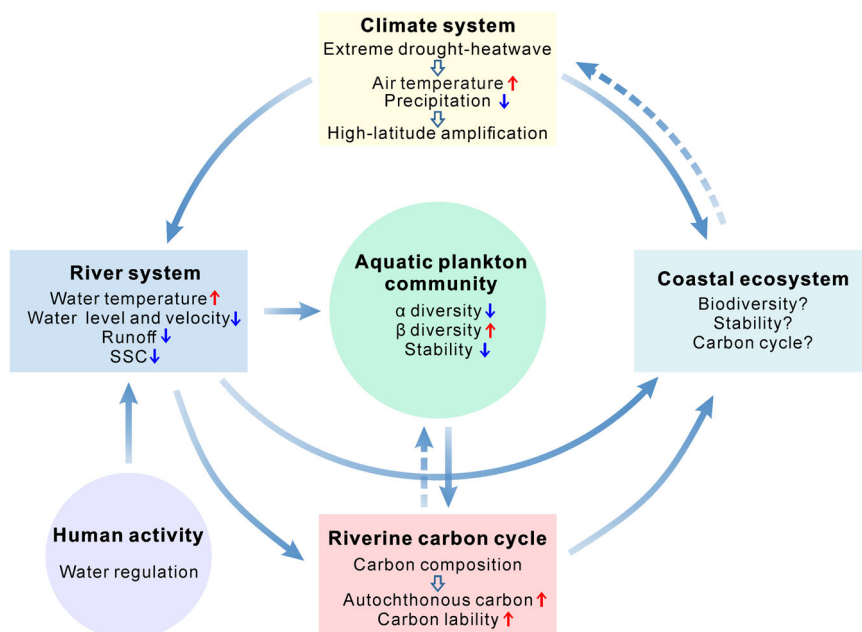
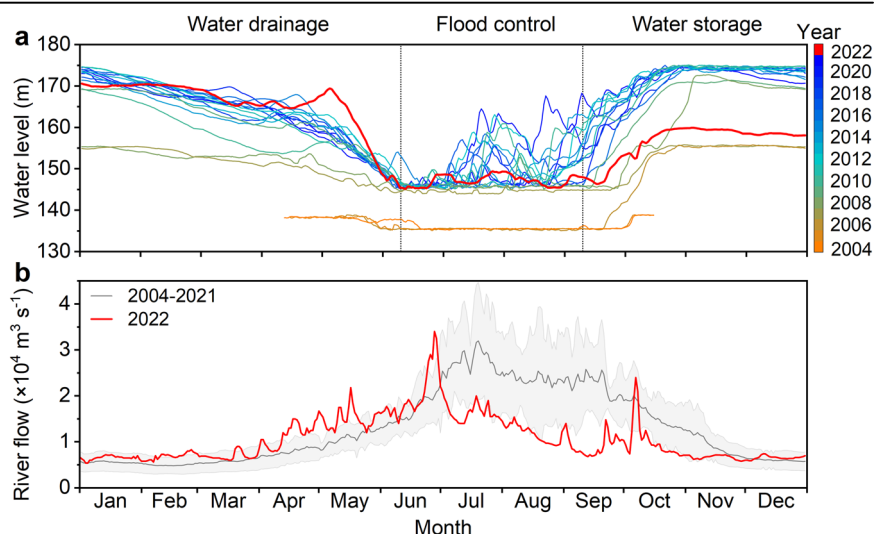


Fig. 10 | Water regime of the Three Gorges Reservoir since its impoundment. **a** Water level. **b** River flow.



copies g^{-1} ; the freeze-dried suspended particulate matter mass was measured using an analytical balance).

Measurement of particulate organic carbon (POC) and labile POC contents

To ensure uniformity, the samples were thoroughly ground using an agate mortar before analysis. This process was conducted to achieve sample homogenization, which is crucial for standardizing preparation and improving the accuracy of subsequent measurements. The homogenized samples were acid-treated with HCl solution (1 M) to completely remove inorganic C before the analysis. The POC and PN contents were determined at Nanjing University using an elemental analyzer (Flash 2000HT, Thermo Fisher Scientific), and the precision of the determination was better than ± 0.02 wt.% and 0.002 wt.%, respectively.

Labile POC was determined following a two-step acid hydrolysis procedure with H_2SO_4 as the extractant, as previously described by

Rovira and Vallejo⁶⁸ and Belay-Tedla et al.⁶⁹. At first, 500 mg of the decarbonated sample was hydrolyzed with 20 ml of 2.5 M H_2SO_4 at 105 °C for 30 min. The hydrolysate was recovered by centrifugation and decantation. The residue was washed with 20 ml of pure water, and the washing supernatant was added to the hydrolysate. This hydrolysate was regarded as labile pool I. The remaining residue was hydrolyzed with 2 ml of 13 M H_2SO_4 overnight at room temperature under continuous shaking. Afterward, the acid concentration was brought down to 1 M by dilution with pure water, and the sample was hydrolyzed at 105 °C for 3 h with occasional shaking. The second hydrolysate was regarded as labile pool II. Labile pools I and II were combined to obtain the total labile pool.

Hydrogeochemical variables

Hydrogeochemical variables including water temperature (°C), dissolved oxygen ($mg\ L^{-1}$), total phosphorus ($mg\ L^{-1}$), total nitrogen ($mg\ L^{-1}$),

ammonia nitrogen (mg L^{-1}), chemical oxygen demand (mg L^{-1}), biochemical oxygen demand (mg L^{-1}), and pH were obtained from real-time monitoring data of water quality cross-section provided by the China National Environmental Monitoring Centre (<https://www.cnemc.cn>) and analyzed using the standard methods⁷⁰. The hydrogeochemical variables analyzed in this study were obtained from monitoring stations located near each of our sampling sites, and the data were temporally matched to our sampling periods, ensuring consistency in the temporal context of the study. To determine suspended sediment concentration (mg L^{-1}), the samples were freeze-dried; the dry sample mass was then weighted using an analytical balance, and the measured mass was normalized by the sampled water volume to calculate suspended sediment concentration accurately.

Statistical analysis

Bioinformatic analysis was carried out using the Majorbio Cloud platform (<https://cloud.majorbio.com>). Based on the OTUs information, rarefaction curves and alpha diversity indices including observed OTUs, Chao1 richness, ACE richness, Shannon diversity, and Good's coverage were calculated with Mothur v.1.30.1⁷¹. Significant differences in the α diversity were studied using the Kruskal-Wallis test with FDR multiple testing correction.

The similarity among three periods in different taxa was determined by Non-metric Multidimensional Scaling (NMDS) based on Bray-Curtis dissimilarity using the Vegan v.2.5-3 package. Significant differences were studied by Adonis with the Monte Carlo 999 permutations test.

The univariate correlation networks were constructed to explore relationships between taxa⁷². A correlation between two nodes was considered to be statistically robust if Spearman's correlation coefficient was over 0.5 or less than -0.5, and the *P*-value less than 0.05. The edge number, average neighbor number, density, clustering coefficient, and modularity of the community network were determined using the "Analyze Network" function in Cytoscape v.3.10.2.

Statistical differences in POC content, labile POC proportion, water temperature, $\text{NH}_3\text{-N}$ concentration, TP concentration, and TN concentration among the water drainage, water storage, and extreme drought-heatwave periods were assessed using the one-way analysis of variance (ANOVA) test in Origin v.2023. Before conducting the one-way ANOVA test, we used the Levene test for homoscedasticity and the Shapiro-Wilk test for the normal distribution. To analyze significant differences in gene quantity across the three periods that did not follow the normal distribution, the Kruskal-Wallis test was performed, using Origin v.2023b.

Data availability

The raw eukaryote sequence data used in this study have been deposited in the NCBI SRA database under accession code PRJNA1221869. The raw prokaryote sequence data used in this study have been deposited in the NCBI SRA database under accession code PRJNA1221784.

Received: 20 August 2024; Accepted: 18 February 2025;

Published online: 01 March 2025

References

- Casas-Ruiz, J. P. et al. Integrating terrestrial and aquatic ecosystems to constrain estimates of land-atmosphere carbon exchange. *Nat. Commun.* **14**, 1571 (2023).
- Hotchkiss, E. et al. Sources of and processes controlling CO₂ emissions change with the size of streams and rivers. *Nat. Geosci.* **8**, 696–699 (2015).
- Rosentreter, J. A. et al. Half of global methane emissions come from highly variable aquatic ecosystem sources. *Nat. Geosci.* **14**, 225–230 (2021).
- Grill, G. et al. Mapping the world's free-flowing rivers. *Nature* **569**, 215–221 (2019).
- Li, F. et al. Environmental DNA biomonitoring reveals the interactive effects of dams and nutrient enrichment on aquatic multitrophic communities. *Environ. Sci. Technol.* **56**, 16952–16963 (2022).
- Vörösmarty, C. J. & Sahagian, D. Anthropogenic disturbance of the terrestrial water cycle. *Bioscience* **50**, 753–765 (2000).
- Best, J. & Darby, S. E. The pace of human-induced change in large rivers: Stresses, resilience, and vulnerability to extreme events. *One Earth* **2**, 510–514 (2020).
- Coronese, M., Lamperti, F., Keller, K., Chiaromonte, F. & Roventini, A. Evidence for sharp increase in the economic damages of extreme natural disasters. *Proc. Natl. Acad. Sci.* **116**, 21450–21455 (2019).
- Perkins-Kirkpatrick, S. & Lewis, S. Increasing trends in regional heatwaves. *Nat. Commun.* **11**, 3357 (2020).
- Sabater, S. et al. Extreme weather events threaten biodiversity and functions of river ecosystems: evidence from a meta-analysis. *Biol. Rev.* **98**, 450–461 (2023).
- Bevacqua, E., Zappa, G., Lehner, F. & Zscheischler, J. Precipitation trends determine future occurrences of compound hot-dry events. *Nat. Clim. Change* **12**, 350–355 (2022).
- Lim, E.-P. et al. Australian hot and dry extremes induced by weakenings of the stratospheric polar vortex. *Nat. Geosci.* **12**, 896–901 (2019).
- Zhang, P. et al. Abrupt shift to hotter and drier climate over inner East Asia beyond the tipping point. *Science* **370**, 1095–1099 (2020).
- Yin, J. et al. Future socio-ecosystem productivity threatened by compound drought-heatwave events. *Nat. Sustain.* **6**, 259–272 (2023).
- Mazdiyasni, O. & AghaKouchak, A. Substantial increase in concurrent droughts and heatwaves in the United States. *Proc. Natl. Acad. Sci. USA* **112**, 11484–11489 (2015).
- Peterson, T. J., Saft, M., Peel, M. C. & John, A. Watersheds may not recover from drought. *Science* **372**, 745–749 (2021).
- Zscheischler, J. et al. A typology of compound weather and climate events. *Nat. Rev. Earth Environ.* **1**, 333–347 (2020).
- Falkowski, P. G., Barber, R. T. & Smetacek, V. V. Biogeochemical Controls and Feedbacks on Ocean Primary Production. *Science* **281**, 200–207 (1998).
- Lampert W., Sommer U. *Limnology: the ecology of lakes and streams*. Oxford University Press (2007).
- Reynolds C. S. *The ecology of phytoplankton*. Cambridge University Press (2006).
- Paerl, H. W. & Paul, V. J. Climate change: links to global expansion of harmful cyanobacteria. *Water Res.* **46**, 1349–1363 (2012).
- Daufresne, M., Lengfellner, K. & Sommer, U. Global warming benefits the small in aquatic ecosystems. *Proc. Natl. Acad. Sci. USA* **106**, 12788–12793 (2009).
- Wernberg, T. et al. An extreme climatic event alters marine ecosystem structure in a global biodiversity hotspot. *Nat. Clim. Change* **3**, 78–82 (2013).
- Bond, N. R., Lake, P. S. & Arthington, A. H. The impacts of drought on freshwater ecosystems: an Australian perspective. *Hydrobiologia* **600**, 3–16 (2008).
- Kingsford, R. T., Bino, G. & Porter, J. L. Continental impacts of water development on waterbirds, contrasting two Australian river basins: Global implications for sustainable water use. *Glob. Chang. Biol.* **23**, 4958–4969 (2017).
- Udall, B. & Overpeck, J. The twenty-first century Colorado River hot drought and implications for the future. *Water Resour. Res.* **53**, 2404–2418 (2017).
- MWRC. *Sediment Communiqué of Chinese Rivers*. China Water & Power Press, Beijing (1990–2022).
- Mallapaty, S. China's extreme weather challenges scientists studying it. *Nature* **609**, 888 (2022).
- Guo, L. et al. From the headwater to the delta: A synthesis of the basin-scale sediment load regime in the Changjiang River. *Earth-Sci. Rev.* **197**, 102900 (2019).

30. Li, G. et al. Dam-triggered organic carbon sequestration makes the Changjiang (Yangtze) river basin (China) a significant carbon sink. *J. Geophys. Res.: Biogeosci.* **120**, 39–53 (2015).
31. Wang, J. et al. Molecular biogeography of planktonic and benthic diatoms in the Yangtze River. *Microbiome* **7**, 1–15 (2019).
32. Paerl, H. W. & Huisman, J. Climate change: a catalyst for global expansion of harmful cyanobacterial blooms. *Environ. Microbiol. Rep.* **1**, 27–37 (2009).
33. Huisman J., Matthijs H., Visser P. Harmful Cyanobacteria Springer Aquatic Ecology Series 3. Dordrecht, The Netherlands, (2005).
34. Diaz, R. J. & Rosenberg, R. Spreading dead zones and consequences for marine ecosystems. *Science* **321**, 926–929 (2008).
35. Qin, B. et al. Extreme climate anomalies enhancing cyanobacterial blooms in eutrophic Lake Taihu, China. *Water Resour. Res.* **57**, e2020WR029371 (2021).
36. Elser, J. J. et al. Global analysis of nitrogen and phosphorus limitation of primary producers in freshwater, marine and terrestrial ecosystems. *Ecol. Lett.* **10**, 1135–1142 (2007).
37. Cardinale, B. J. et al. Biodiversity loss and its impact on humanity. *Nature* **486**, 59–67 (2012).
38. Loreau, M. et al. Biodiversity and ecosystem functioning: current knowledge and future challenges. *Science* **294**, 804–808 (2001).
39. Hillebrand, H., Bennett, D. M. & Cadotte, M. W. Consequences of dominance: a review of evenness effects on local and regional ecosystem processes. *Ecology* **89**, 1510–1520 (2008).
40. Bogan, M. T., Boersma, K. S. & Lytle, D. A. Resistance and resilience of invertebrate communities to seasonal and suprasedonal drought in arid-land headwater streams. *Freshw. Biol.* **60**, 2547–2558 (2015).
41. Mosley, L. M. Drought impacts on the water quality of freshwater systems; review and integration. *Earth-Sci. Rev.* **140**, 203–214 (2015).
42. Woodward, G., Perkins, D. M. & Brown, L. E. Climate change and freshwater ecosystems: impacts across multiple levels of organization. *Philos. Trans. R. Soc. B: Biol. Sci.* **365**, 2093–2106 (2010).
43. Yuan, D. et al. High temperature induced metabolic reprogramming and lipid remodeling in a high-altitude fish species, *Triplophysa bleekeri*. *Front. Mar. Sci.* **9**, 1017142 (2022).
44. Huo, D., Gaitán-Espitia, J. D., Spicer, J. I. & Yang, H. The adaptation and response of aquatic animals in the context of global climate change. (eds Huo, D., Gaitán-Espitia, J. D., Spicer, J. I. & Yang, H.). *Front. Media SA* **10**, 1231099 (2023).
45. Gilbertson C. Aquaculture industry resilience against climate change: examining the effects of mild stress on heat tolerance in juvenile Chinook salmon (*Oncorhynchus tshawytscha*). (2022).
46. Montoya, J. M., Pimm, S. L. & Solé, R. V. Ecological networks and their fragility. *Nature* **442**, 259–264 (2006).
47. Allesina, S. & Tang, S. Stability criteria for complex ecosystems. *Nature* **483**, 205–208 (2012).
48. Chen, Y. River ecosystem metabolism and carbon cycling. *Nat. Water* **1**, 224–224 (2023).
49. Krause-Jensen, D. & Duarte, C. M. Substantial role of macroalgae in marine carbon sequestration. *Nat. Geosci.* **9**, 737–742 (2016).
50. Bernhardt, E. S. et al. Light and flow regimes regulate the metabolism of rivers. *Proc. Natl. Acad. Sci.* **119**, e2121976119 (2022).
51. Jiang, J. et al. Extreme drought-heatwave exacerbates water quality deterioration in China. *Ecol. Indic.* **170**, 113008 (2025).
52. Ni, J. et al. Three Gorges Dam: friend or foe of riverine greenhouse gases? *Natl. Sci. Rev.* **9**, nwac013 (2022).
53. Zhang, Y. et al. Terrigenous organic carbon drives methane dynamics in cascade reservoirs in the upper Yangtze China. *Water Res.* **219**, 118546 (2022).
54. Sarthou, G., Timmermans, K. R., Blain, S. & Tréguer, P. Growth physiology and fate of diatoms in the ocean: a review. *J. Sea Res.* **53**, 25–42 (2005).
55. Litchman, E., Klausmeier, C. A., Schofield, O. M. & Falkowski, P. G. The role of functional traits and trade-offs in structuring phytoplankton communities: scaling from cellular to ecosystem level. *Ecol. Lett.* **10**, 1170–1181 (2007).
56. Paerl, H. W. & Otten, T. G. Harmful cyanobacterial blooms: causes, consequences, and controls. *Micro. Ecol.* **65**, 995–1010 (2013).
57. Paerl, H. W. & Huisman, J. Blooms like it hot. *Science* **320**, 57–58 (2008).
58. Heisler, J. et al. Eutrophication and harmful algal blooms: a scientific consensus. *Harmful Algae* **8**, 3–13 (2008).
59. Sejr M. K., Poste A. E. & Renaud P. E. Multiple climatic drivers increase pace and consequences of ecosystem change in the Arctic Coastal Ocean. *Limnology Oceanography Lett.* **9**, 683–695 (2024).
60. Schuur, E. A. et al. Climate change and the permafrost carbon feedback. *Nature* **520**, 171–179 (2015).
61. Natali, S. M. et al. Large loss of CO₂ in winter observed across the northern permafrost region. *Nat. Clim. Change* **9**, 852–857 (2019).
62. Hicks Pries, C. E. et al. Decadal warming causes a consistent and persistent shift from heterotrophic to autotrophic respiration in contrasting permafrost ecosystems. *Glob. Change Biol.* **21**, 4508–4519 (2015).
63. Palmer, M. A. et al. Climate change and river ecosystems: protection and adaptation options. *Environ. Manag.* **44**, 1053–1068 (2009).
64. Palmer, M. A. et al. Climate change and the world's river basins: anticipating management options. *Front. Ecol. Environ.* **6**, 81–89 (2008).
65. Hua, W., Dai, A., Qin, M., Hu, Y. & Cui, Y. How unexpected was the 2022 summertime heat extremes in the middle reaches of the Yangtze River? *Geophys. Res. Lett.* **50**, e2023GL104269 (2023).
66. Brâte, J. et al. Freshwater Perkinsea and marine-freshwater colonizations revealed by pyrosequencing and phylogeny of environmental rDNA. *ISME J.* **4**, 1144–1153 (2010).
67. Nübel, U., Garcia-Pichel, F. & Muyzer, G. PCR primers to amplify 16S rRNA genes from cyanobacteria. *Appl. Environ. Microbiol.* **63**, 3327–3332 (1997).
68. Rovira, P. & Vallejo, V. R. Labile and recalcitrant pools of carbon and nitrogen in organic matter decomposing at different depths in soil: an acid hydrolysis approach. *Geoderma* **107**, 109–141 (2002).
69. Belay-Tedla, A., Zhou, X., Su, B., Wan, S. & Luo, Y. Labile, recalcitrant, and microbial carbon and nitrogen pools of a tallgrass prairie soil in the US Great Plains subjected to experimental warming and clipping. *Soil Biol. Biochem.* **41**, 110–116 (2009).
70. State Environmental Protection Administration. *Water and wastewater monitoring analysis method of editorial committee: Water and wastewater monitoring analysis method, 4th.* China Environmental Science Press, Beijing (2002).
71. Schloss, P. D. et al. Introducing mothur: open-source, platform-independent, community-supported software for describing and comparing microbial communities. *Appl. Environ. Microbiol.* **75**, 7537–7541 (2009).
72. Barberán, A., Bates, S. T., Casamayor, E. O. & Fierer, N. Using network analysis to explore co-occurrence patterns in soil microbial communities. *ISME J.* **6**, 343–351 (2012).

Acknowledgements

This research was funded by the National Natural Science Foundation of China (42276170, 42293261, and 42106158) and the Fundamental Research Funds for the Central Universities (14380100). We thank Zhenyu Zhang, Zhimin Zhang, Shaojian Huang, and Peng Zhang for sampling. No specific permissions were required for sampling in this study.

Author contributions

J. H.G., Y.S., and J.X.L. designed the study. J.X.L., T.L., S.J.L., Y.B.Q., S.Z., and D.P. conducted the sampling. J.X.L., T.L., and G.Y. performed the experiments. J.X.L. interpreted the data and wrote the

manuscript. J. H.G., Y.X.Z., and X.M.X. contributed discussion. C.H.C. provided assistance with figures. All authors contributed to the final version.

Competing interests

The authors declare no competing interests.

Additional information

Supplementary information The online version contains supplementary material available at

<https://doi.org/10.1038/s43247-025-02143-1>.

Correspondence and requests for materials should be addressed to Jianhua Gao.

Peer review information *Communications Earth and Environment* thanks the anonymous reviewers for their contribution to the peer review of this work. Primary Handling Editors: José Luis Iriarte Machuca, Somapama Ghosh[A peer review file is available.]

Reprints and permissions information is available at <http://www.nature.com/reprints>

Publisher's note Springer Nature remains neutral with regard to jurisdictional claims in published maps and institutional affiliations.

Open Access This article is licensed under a Creative Commons Attribution-NonCommercial-NoDerivatives 4.0 International License, which permits any non-commercial use, sharing, distribution and reproduction in any medium or format, as long as you give appropriate credit to the original author(s) and the source, provide a link to the Creative Commons licence, and indicate if you modified the licensed material. You do not have permission under this licence to share adapted material derived from this article or parts of it. The images or other third party material in this article are included in the article's Creative Commons licence, unless indicated otherwise in a credit line to the material. If material is not included in the article's Creative Commons licence and your intended use is not permitted by statutory regulation or exceeds the permitted use, you will need to obtain permission directly from the copyright holder. To view a copy of this licence, visit <http://creativecommons.org/licenses/by-nc-nd/4.0/>.

© The Author(s) 2025